Connections between the energy functional and interaction potentials for materials simulations

Christopher D. Taylor*
Materials Technology–Metallurgy (MST-6), Materials Science and Technology Division, Los Alamos National Laboratory, Los Alamos, New Mexico 87545, USA

(Received 18 November 2008; revised manuscript received 17 April 2009; published 7 July 2009)

In this work it is shown that the energy of a material can be expressed as a functional of the atomic density distribution function and that this energy can be approximated via the method of Taylor expansion. It is then shown that a matrix representation of the second-order term in the Taylor expansion of the energy functional provides a parameterizable expression for the energy that avoids the necessity of finding the as yet unknown functional forms connecting atomic positions to system energies. Using the basis of spherical harmonics $\{Y_{lm}\}$ it is shown that the matrix representation of the energy involves the computation of the Steinhardt bond-orientational order parameters, previously used to classify local crystallographic orderings in amorphous materials. It is also shown that these parameters coincide with the "embedding density" corrections utilized in the modified embedded atom method. By incorporating these bond-orientational order parameters into the Taylor expansion for the energy function, it is demonstrated that this method provides a means for reproducing the phase diagram of various metallic states of Cu and U. Consequently, the formalism introduced here is demonstrated to be systematically improvable via improvements in the underlying basis set of spherical harmonics. Finally, it is shown by reference to the body-centered cubic phase of U that extension to arbitrary crystallographic requires a further examination of the use of interatomic screening potentials that "dampen" the contributions of atoms other than first-nearest neighbors.

DOI: 10.1103/PhysRevB.80.024104 PACS number(s): 61.50.Ah, 61.66.Bi

I. MOTIVATION

Although Moore's Law has continued to hold true in the realm of computational performance, it has been argued that an analogous exponentiation of progress has not manifested in the realm of interaction potentials for materials simulation.[1] The considerable achievements made, therefore, in computing capabilities cannot be fully exploited to provide commensurate advances in our understanding of materials until rigorous techniques for constructing such interaction potentials are established and aggressively developed. In this work we propose one possible general framework for such a materials interaction potential operating at the atomic (but not electronic) level and subsequently derive some specific instances of this materials interaction potential that may be suitable for molecular dynamics or Monte Carlo simulations of materials. The resulting materials interaction potentials, by virtue of the proposed method of construction, possess an accuracy that is systematically improvable through the addition of higher-order terms in a Taylor expansion or expansion of the basis set upon which the atomic density distribution (obtained from the coordinates of each of the atoms in a simulation, for example, or a thermal probability distribution obtained from experiment) is represented.

The current set of materials interaction potentials can be broadly separated into three main classes: pair potentials, embedding potentials, and self-consistent potentials. Pair potential techniques are typically extensions of empirical relations derived for materials interactions under a given set of circumstances.[2–4] Rarely do pair potentials offer the opportunity for rigorous and systematic improvements in predictive performance, due to their specificity to a certain class of interaction, or a lack of theoretical sophistication in their underlying functional forms. For any given material there is typically a fusion of various interaction classes (ionic, covalent, van der Waals, metallic) that are operative, and their exact combination may vary with conditions of strain, distortion or local impurity content.

Embedding methods are conceptually rooted within the fundamental forms provided by density-functional theory (DFT),[5] however, these connections are rarely made explicit and quantitative. Instead, embedding energy functional forms, including not only the embedded atom method (EAM), but the equivalent crystal method and the effective medium theory, tend to spring from a sense of chemical or physical intuition rather than rigorous and extensible representations.[6–10] The following work will go some way to demonstrate an alternative approach to the derivation of embedding methods.

Self-consistent methods, such as the tight binding, bond order, and ReaxFF potentials, are often the most computationally intensive, rooted as they are in solving simplified Hamiltonian eigenequations.[11–13] Self-consistent methods typically offer extensible physics, such that, with additional computational expense, the energies and properties obtained can be systematically improved.[14]

While self-consistent methods offer one avenue toward improved materials interaction potentials, we posit that such self-consistent methods operate on a higher level than is desirable for many atomistic materials simulations, and that less demanding yet still extensible methods can be derived by exploiting the fundamental premises underlying the Landau theory for second-order phase transitions. These premises include (a) that the energy may be written as a functional of the atomic density distribution (corresponding to the distribution of the positions of the nuclei, and not, therefore, directly related to the electronic structure), (b) that the functional can be approximated by the first few terms of a Taylor expansion, and (c) that the atomic density distribution

can be represented in a basis of symmetry-adapted functions.[15]

In this paper we first outline a general expression for the energy of a system in terms of the distribution of atoms in the system, and decompose this into a sum of localized embedding forms. By representing the atomic distribution in terms of some suitable basis, it is shown that the energy can be determined from a knowledge of the interaction energies coupling these basis functions with one another. It will then be shown how the basis of spherical harmonics leads to an expression of the energy in terms of the bond-orientational order parameters,[16] and this has close parallels to elements contained within the modified embedded atom method (MEAM).[9] Furthermore, it will be shown that various existing interatomic potentials taken from the three classes discussed are compatible with this particular representation. Finally a demonstration of this technique will be made for the cases of copper and uranium metals, whereby the appropriate parameters are determined from a set of first-principles strain-energy relations computed for various crystal structures. Pathways for future development of this particular model are then discussed.

II. GENERAL FORMS

A. Energy functional and approximations to the energy functional

Landau's theory of second-order phase transitions begins with the expression of a crystal structure in terms of the atomic density distribution function $\rho(\mathbf{r})$.[15] The energy of a system, E, is then expressed as a functional of $\rho(\mathbf{r})$

$$E = \Phi[\rho(\mathbf{r})] \tag{1}$$

For the purposes of a classical molecular dynamics simulation, the atomic density distribution function, at any moment in time, is given as a sum of Dirac delta functions over the atomic coordinates, $\mathbf{r_j}$

$$\rho(\mathbf{r}) = \sum_i \delta(\mathbf{r} - \mathbf{r_i}) \tag{2}$$

For the analysis of experimentally determined densities, which may be thermally smeared, alternative representations of the density can be used; a sum of Gaussian distribution functions, for example. Even more generally, the atomic density distribution function may be given as a set of such functions, each representing the distribution associated with elements of a given atomic number Z and/or electronic state (i.e., charged or excited atoms may have different dependencies compared to neutral atoms). In analogy to DFT, the "external potential" $v(\mathbf{r})$ exerted by the nuclei could also be used. We omit these possibilities for now, although it will be necessary to develop these concepts in future work.

Given some ground-state atomic density distribution function $\rho_0(\mathbf{r})$ with energy E_0, the energy of a related state having atomic density distribution function $\rho(\mathbf{r}) = \rho_0(\mathbf{r}) + \delta\rho(\mathbf{r})$ can be expressed as a Taylor series[17]

$$E = E_0 + \int\int \frac{\partial^2\Phi}{\partial\rho^2}(r,r')\,\delta\rho(\mathbf{r})\,\delta\rho(\mathbf{r}')\,d\mathbf{r}d\mathbf{r}' + \ldots \tag{3}$$

The first-order term disappears because we have assumed that we are starting with the ground-state density $\rho_0(\mathbf{r})$. The Taylor series representation is advantageous since it provides us with a basic framework from which approximate methods for determining the energy of a system can be derived, while maintaining a mechanism by which the energy may be systematically improved (i.e., by adding higher-order terms).

Inserting the expression for $\rho(\mathbf{r})$ from Eq. (2) into Eq. (3) produces the following to second order

$$E = E_0 + \int\int \frac{\partial^2\Phi}{\partial\rho^2}(r,r')\left\{\sum_i [\delta(\mathbf{r} - \mathbf{r_i}) - \delta(\mathbf{r} - \mathbf{r_i^0})]\right\} \times\left[\sum_j \delta(\mathbf{r}' - \mathbf{r_j}) - \delta(\mathbf{r}' - \mathbf{r_j^0})\right] d\mathbf{r}d\mathbf{r}' \tag{4}$$

where the $\mathbf{r_i^0}$ are the coordinates of the atoms in the ground-state configuration. The Dirac delta functions reduce Eq. (4) to

$$E = E_0 + \sum_{i,j} \frac{\partial^2\Phi}{\partial\rho^2}(\mathbf{r_i},\mathbf{r_j}) - \frac{\partial^2\Phi}{\partial\rho^2}(\mathbf{r_i^0},\mathbf{r_j}) - \frac{\partial^2\Phi}{\partial\rho^2}(\mathbf{r_i},\mathbf{r_j^0}) + \frac{\partial^2\Phi}{\partial\rho^2}(\mathbf{r_i^0},\mathbf{r_j^0}) \tag{5}$$

By introducing the following shorthand

$$f(\mathbf{r_i},\mathbf{r_j}) = \frac{\partial^2\Phi}{\partial\rho^2}(\mathbf{r_i},\mathbf{r_j})g(\mathbf{r_j}) = \sum_i \frac{\partial^2\Phi}{\partial\rho^2}(\mathbf{r_i^0},\mathbf{r_j}), \tag{6}$$

assuming that

$$\frac{\partial^2\Phi}{\partial\rho^2}(\mathbf{r_i^0},\mathbf{r_j}) = \frac{\partial^2\Phi}{\partial\rho^2}(\mathbf{r_j},\mathbf{r_i^0}) \tag{7}$$

and subsuming the final term into the constant E_0, Eq. (5) reduces to a sum of one- and two-body terms

$$E = E_0 + \sum_i g(\mathbf{r_i}) + \sum_{i,j} f(\mathbf{r_i},\mathbf{r_j}). \tag{8}$$

The representation of the energy in terms of one- and two-body terms is fundamental to a number of materials interaction potential schemes, as best expressed by the concepts developed by Stott and Zaremba.[18] The outstanding problem, tackled in various ways and with varying levels of success, is to "discover" the forms of these functions $g(\mathbf{r})$ and $f(\mathbf{r},\mathbf{r}')$.

In the following we shall show that, by eschewing the delta function representation of the atomic coordinates in favor of some suitable basis, we may bypass the "hard problem" posed by the unknown functions, $f(\mathbf{r},\mathbf{r}')$ and $g(\mathbf{r})$. Before so doing, however, it is instructive to consider how the energy functional of the *atomic* density distribution function in Eq. (1) relates to functionals of the *electron* density distribution function, as developed in the Hohenberg-Kohn DFT.[19]

B. Connections to electronic structure theory

The first Hohenberg-Kohn theorem states that the ground-state properties of a many electron system may be uniquely

determined by the spatial one-electron density distribution function $\rho_e(\mathbf{r})$.[19] Thus, in analogy to Eq. (1), the Hohenberg-Kohn theorem establishes that there exists a functional Φ_e that determines the energy associated with a given electron-density distribution function $\rho_e(\mathbf{r})$

$$E = \Phi_e[\rho_e(\mathbf{r})] \tag{9}$$

As a means to this end, Hohenberg and Kohn also established that there is a one-to-one correspondence between the external potential $v_{\text{ext}}(\mathbf{r})$ and the ground-state electron distribution $\rho_e(\mathbf{r})$, for a given number of electrons N_e. Thus $\rho_e(\mathbf{r})$ may also be expressed as a functional $\mathcal{V}$ of $v_{\text{ext}}(\mathbf{r})$ given N_e.

$$\rho_e(\mathbf{r}) = \mathcal{V}[v_{ext}(\mathbf{r}'), N_e] \tag{10}$$

In atomic systems, $v_{\text{ext}}(\mathbf{r})$ most commonly derives from the positions of the nuclei expressed here as the atomic density distribution function $\rho(\mathbf{r})$ via the Poisson equation, although additional external potentials $v_{\text{ext}'}(\mathbf{r})$ may apply also (electromagnetic fields, for instance). Hence, the electronic distribution can ultimately be determined (in a nontrivial way as specified by the functional $\mathcal{V}'$) from the atomic density distribution function $\rho(\mathbf{r})$ and any additional potential $v_{\text{ext}'}(\mathbf{r})$

$$\rho_e(\mathbf{r}) = \mathcal{V}'[\rho(\mathbf{r}'), v_{\text{ext}'}(\mathbf{r}'), N_e] \tag{11}$$

Insertion of this equation into Eq. (9) reveals that the energy can ultimately be expressed as a functional of this atomic density distribution, plus any additional potentials not resulting from electrostatic interaction with the nuclei, for a given number of electrons N_e. By including these last two features of the problem into the specific functional Φ we arrive at the original expression from Landau, Eq. (1)

$$E = \Phi_e\{\mathcal{V}'[\rho(\mathbf{r}), v_{\text{ext}'}(\mathbf{r}), N_e]\} = \Phi[\rho(\mathbf{r})]|_{N_e, v_{\text{ext}'}} \tag{12}$$

Thus it can be demonstrated from quantum mechanics that the ground-state energy for an atomic system may be directly computed as a functional of the atomic density distribution, given a certain external potential $v_{\text{ext}'}(\mathbf{r})$ and number of electrons, N_e.

III. EMBEDDED FORMS

In this section we consider the computation of the energy from a localized, or *embedded* perspective, in that computation of the energy is broken down into a sum of individual atomic energies.[18] This localization is achieved by creating local representations of the total atomic density distribution function, such that energy calculations may be efficiently performed with 'order N' scaling, where N is the number of atoms.

Consider now a particular atom i within the total atomic density distribution function $\rho(\mathbf{r})$. The embedding concept implies a localization of energy, based upon the neighborhood "sensed" by that atom i. We define a local atomic distribution density as

$$\rho_i(\mathbf{r}) = \sum_{j \neq i} \delta(\mathbf{r} - \mathbf{r_j}) w(r_{ij}) \tag{13}$$

Here the sum is over all atoms $j \neq i$ and the Dirac delta function is weighted by the expression $w(r_{ij})$. The weighting function may be a simple cut-off function, or a more complex type of screening function, such as the elliptical screening introduced by Baskes.[9] The sum over the local atomic density distribution functions $\rho_i(\mathbf{r})$ may not necessarily add up to the total $\rho(\mathbf{r})$.

We may express the local, or *embedding*, energy E_i as a perturbation from some initial energy E_0^i based upon a reference configuration $\rho_i^0(\mathbf{r})$ in the same way as the more general energy in Eq. (3). Omitting the intermediate steps, which parallel those above, we arrive at an analogous expression to Eq. (8)

$$E_i = E_0^i + \sum_{j \neq i} g_i(\mathbf{r_j}) w(r_{ij}) + \sum_{j \neq i, k \neq i} f_i(\mathbf{r_j}, \mathbf{r_k}) w(r_{ij}) w(r_{ik}) \tag{14}$$

Using this embedding formalism, therefore, the second-order expression for the energy has been assumed to adopt a localized form, consisting of the weighted interactions between an atom and its neighbors, and the atom and pairs taken from the neighbors.

It is instructive to consider the correspondence between the embedding energy given in Eq. (14) and the total energy from Eq. (8), as this will provide some guidance as to the reasonableness of the localization assumption implicit in the embedding formalism. If we assume that the total energy is given as the sum over the localized, atom centered embedding energies we have, to second order

$$E_{tot} \approx \sum_i E_0^i + \sum_{i, j \neq i} g_i(\mathbf{r_j}) w(r_{ij}) + \sum_{i, j \neq i, k \neq i} f_i(\mathbf{r_j}, \mathbf{r_k}) w(r_{ij}) w(r_{ik}) \tag{15}$$

and thus the correspondences exist

$$f(\mathbf{r_i}, \mathbf{r_j}) \equiv \sum_k f_k(\mathbf{r_i}, \mathbf{r_j}) w(r_{ik}) w(r_{jk}) g(\mathbf{r_i}) \equiv \sum_j g_j(\mathbf{r_i}) w(r_{ij}) \tag{16}$$

The latter relation can be understood in the light of the original definition of $g(\mathbf{r_i})$ [from Eq. (5)] as the interaction of the atom positions $\{\mathbf{r_i}\}$ with the reference positions $\{\mathbf{r_j^0}\}$; the reference atoms j in $g_j(\mathbf{r_i})$ provide a center from which the deviation contained in $\mathbf{r_i}$ from the reference material can be determined. Likewise the two-body energy $f(\mathbf{r_i}, \mathbf{r_j})$ has been mapped to a series of weighted two-body interactions as "assessed" from the standpoint of a reference atom k. In principle, given suitable forms for $f_k(\mathbf{r_i}, \mathbf{r_j})$ and the weighting functions $w(r_{ij})$ these relations could be made exact. Unfortunately exact knowledge of these functional forms is elusive, and alternative approaches have to be made. At the same time, even long-range forces such as the Coulombic interaction have been shown to be effectively local given appropriate choices of $w(r_{ij})$.[20]

In the following an alternative and more useful methodology shall be introduced that bypasses these unknown func-

tions $f(\mathbf{r_i},\mathbf{r_j})$ and $g(\mathbf{r_i})$, but rather harkens directly back to Eq. (3) by using representations of the local atomic density distribution in terms of some basis $\{\chi_j(\mathbf{r})\}$.

IV. MATRIX FORMULATION

Expressing the local atomic density distribution function $\rho_i(\mathbf{r})$ in terms of some basis $\{\chi_j(\mathbf{r})\}$ enables a matrix formulation for the embedding energy E_i. In doing so we continue the tradition of Landau by utilizing appropriate symmetry representations of the atomic density distribution.[15] By defining the order parameter

$$c_j = \int \rho_i(\mathbf{r})\chi_j^*(\mathbf{r})d\mathbf{r} \tag{17}$$

then

$$\rho_i(\mathbf{r}) \approx \sum_j c_j\chi_j(\mathbf{r}) \tag{18}$$

This relation is exact if the basis $\{\chi_j\}$ is complete.

Defining $\{c_j^0\}$ as the set of expansion coefficients for the reference configuration and inserting this representation of the density in Eq. (3), the energy to second order becomes

$$E_i = E_0^i + \int\int \frac{\partial^2\Phi}{\partial\rho^2}(\mathbf{r},\mathbf{r}')\sum_j (c_j - c_j^0)\chi_j(\mathbf{r})\sum_k (c_k - c_k^0)\chi_k(\mathbf{r}')d\mathbf{r}d\mathbf{r}' = E_0^i + \sum_{j,k}(c_j - c_j^0)(j|\mathcal{F}|k)(c_k - c_k^0) \tag{19}$$

where we have defined the operator $\mathcal{F}$ as $\frac{\partial^2\Phi}{\partial\rho^2}(\mathbf{r},\mathbf{r}')$ and introduced the following convenient notation

$$(j|\mathcal{F}|k) = \int\int \frac{\partial^2\Phi}{\partial\rho^2}(\mathbf{r},\mathbf{r}')\chi_j(\mathbf{r})\chi_k(\mathbf{r}')d\mathbf{r}d\mathbf{r}' \tag{20}$$

In this way an intelligent basis decomposition of the local atomic density distribution function allows approximations to the energy to be efficiently computed in terms of the coefficients, $\{c_j\}$ and the constants F_{jk} present in the matrix representation $\mathbf{F}$ of $\mathcal{F}$, suitably parameterized for a given atom type. The functions $f(\mathbf{r_i},\mathbf{r_j})$ and $g(\mathbf{r_i})$ are now contained within this matrix representation and thus their explicit form need not be determined. We shall now proceed to provide instances of this matrix representation, drawing from the literature pertaining to crystallographic order parameters in particular.[21]

V. REPRESENTATION OF THE LOCAL ATOMIC DENSITY DISTRIBUTION FUNCTION BY THE BOND ORIENTATIONAL ORDER

Bond-orientational order parameters have been applied to the characterization of crystallographies present at the local level of disordered phases, and atomic clusters.[16,21,22] These rotationally invariant parameters are attractive for use in a materials interaction potential since knowledge of the local crystallographic environment can, in many cases, suffice to determine energies in a local way. This thesis is especially relevant to many atomistic systems in which a pair potential or embedding method is used, as these methods typically apply a cutoff for neighborhood determination, and so are inherently local. In addition to this observation, another obvious observation may be added: atoms of differing type (be they atoms of differing atomic number or atoms of the same atomic number yet differing in their electronic states) exhibit differing crystallographic preferences. Thus, iron at room temperature is a body-centered cubic (bcc) metal, whereas platinum is face centered cubic (fcc), zinc is hexagonal closest packed (hcp), uranium is orthorhombic, bismuth is rhombohedral, and plutonium is monoclinic.[23] It therefore seems reasonable to utilize a quantitative metric of the local crystallographic environment in order to describe the deviation of an atom's environment from its preferred state, and thus to determine in a quantitative sense the energy required in order to produce said deviation. In the following we provide a quantitative basis for this "materials intuition" by showing how the bond-orientational order parameter[16] can be derived from the atomic density distribution function based upon the preceding framework.

Bond-orientational order parameters ignore the r dependence of the nearest neighbors (NNs), focusing instead on the angular arrangement of the nearest neighbors, captured by the vectors (ϕ_{ij},θ_{ij}).[16] In order to avoid the obligation to select a preferred set of axes, the parameters are set to be rotationally invariant through normalization, as detailed below. Localization of the bond-orientational order is typically achieved by restricting the sum, for example, to the nearest 12 neighbors. Herein we generalize this choice through the initially unspecified weighting function $w(r_{ij})$. The angular arrangement is characterized by utilizing the basis of spherical harmonics $\{Y_{lm}(\phi,\theta)\}$.

The lm-th moment of an atom is given by the projection of the local atomic density distribution function onto $Y_{lm}(\phi,\theta)$. Using Dirac notation,

$$\mu_{lm,i} = \langle Y_{lm}(\phi,\theta)|\rho_i(r,\phi,\theta)\rangle \tag{21}$$

In this way, $\mu_{lm,i}$ resembles c_j in Eq. (17). Using the definition of $\rho_i(\mathbf{r})$ provided in Eq. (13) $\mu_{lm,i}$ becomes

$$\mu_{lm,i} = \sum_j Y_{lm}(\phi_{ij},\theta_{ij})w(r_{ij}) \tag{22}$$

Furthermore, $\rho_i(\mathbf{r})$ can now be expanded, but with loss of radial information, as

$$\tilde{\rho}_i(\mathbf{r}) = \sum_{lm} \mu_{lm,i}Y_{lm}(\phi,\theta) \tag{23}$$

where the tilde has been used to indicate loss of radial information. $\tilde{\rho}_i(\mathbf{r})$ is the *radially reduced density*. The l-th component of $\tilde{\rho}_i(\mathbf{r})$ can be obtained by projection and summation

$$\tilde{\rho}_{l,i}(\mathbf{r}) = \sum_m |Y_{lm}(\phi,\theta)\rangle\langle Y_{lm}(\phi,\theta)|\rho_i(\mathbf{r})\rangle \tag{24}$$

The norm of this l-frequency component is rotationally invariant, unlike $\mu_{lm,i}$, and corresponds to the Steinhardt bond-orientational order parameter $\mu_{l,i}$ (Ref. 16)

$$\mu_{l,i} = \sqrt{\langle \tilde{\rho}_{l,i}(\mathbf{r}) | \tilde{\rho}_{l,i}(\mathbf{r}) \rangle} = \sqrt{\sum_{j,k} w(r_{ij}) w(r_{ik}) P_l(\cos\ \theta_{jik})} \tag{25}$$

The latter expression in terms of the Legendre polynomials $P_l(\cos\ \theta_{jik})$ arises from the addition theorem for spherical harmonics. We may then write the radially reduced density as a sum of the rotationally invariant l-frequency coefficients, $\mu_{l,i}$ multiplied by the normalized *variant* functions $\tilde{Y}_{l,i}(\phi,\theta)$:[16]

$$\tilde{\rho}_i(\mathbf{r}) = \sum_l \tilde{\rho}_{l,i}(\mathbf{r}) = \sum_l \mu_{l,i} \tilde{Y}_{l,i}(\phi,\theta) \tag{26}$$

Distortions in the radially reduced density from some ground-state orientation having coefficients $\{\mu^0_{l,i}\}$ are given by

$$\delta\tilde{\rho}_i(\mathbf{r}) = \sum_l \mu_{l,i} \tilde{Y}_{l,i}(\phi,\theta) - \mu^0_{l,i} \tilde{Y}^0_{l,i}(\phi,\theta) \tag{27}$$

Kazhdan *et al.*[24] have shown that a lower bound for the norm of $\delta\tilde{\rho}_i(\mathbf{r})$ is given by the norm of the approximation

$$\delta\tilde{\rho}_i(\mathbf{r}) \approx \sum_l (\mu_{l,i} - \mu^0_{l,i}) \tilde{Y}_{l,i}(\phi,\theta) \tag{28}$$

Such an approximation captures, therefore, in a general way the distortions in the local crystallography of the atom, with the omission of any radial dependence that is not already captured by the weighting functions $w(r_{ij})$. While more exact representations may result from consideration of the variant quantities $\mu_{lm,i}$, the increase in parameter space and necessity of adopting a preferred set of axes hinder their application. Kazhdan *et al.* have shown previously that, for the purpose of classifying three-dimensional shapes, the one-dimensional array of rotationally invariant forms $\mu_{l,i}$ in most cases performs better than methods requiring principal axes alignment of the two-dimensional array of rotationally variant coefficients $\mu_{lm,i}$.[24] We therefore adopt this approach, although alternative basis sets $\{\chi_j\}$ may yet provide a more accurate and useful specification of the local atomic density distribution function.

Using this lower bound, then, and assuming that a reduced radial distribution sufficiently captures the local crystallography, the energy of atom i, to second order, may be approximated using Eq. (19)

$$E_i \approx E^i_0 + \sum_{l,l'} (\mu_{l,i} - \mu^0_{l,i})(l|\mathcal{F}|l')(\mu_{l',i} - \mu^0_{l',i}) \tag{29}$$

If we assume that states of different frequency l do not couple under the operator $\mathcal{F}$ (testing for the cases of U and Cu described below showed that this contribution is indeed negligible) we arrive at the radially reduced NMEX equation

$$\tilde{E}_i = E^i_0 + \sum_l F_{ll} (\mu_{l,i} - \mu^0_{l,i})^2 \tag{30}$$

where NMEX is an acronym of neighborhood moment expansion, and is used as the descriptive title for this interatomic potential framework.

It should be clear that this potential could be systematically improved by including higher-order terms l, the effect of coupling between l moments, and/or by including higher-order terms in the Taylor expansion. The cost of these improvements, however, is an increase in the number of parameters that need to be determined for the system at hand. However, with the present ability to generate a large number of high quality, hypothetical structures using density-functional theory, for example, the development of parameters can be achieved without too much worry about over training a parameter set to a small number of training structures. Since the art of parameterization is not presently the focus of this work we defer the reader to other works on that topic such as the Bayesian analysis of interatomic potentials for Mo performed by Frederiksen *et al.*[25]

VI. RESTORING RADIAL DEPENDENCE TO THE REPRESENTATION OF THE LOCAL ATOMIC DENSITY DISTRIBUTION FUNCTION

In this section, the definition of the bond-orientational order is modified so as to better represent the local atomic density distribution function such that radial dependence is not neglected. In doing so, the framework for a more exact symmetry representation is established for use in NMEX simulations of materials.

A. Augmenting the functional forms

Let the functional representation $\{\chi_j(\mathbf{r})\}$ introduced in Eq. (17) correspond to the lm spherical harmonics, except now with the incorporation of a radial function $f_l(r)$ which may be unique for each value of l

$$\chi_{lm}(\mathbf{r}) = f_l(r) Y_{lm}(\phi,\theta) \tag{31}$$

This decoupling of the radial and angular dependencies represents an approximation to the functional form, but not an uncommon one. Additionally, assuming that the $(2l+1)$ components of each frequency l share the same radial dependence embodies another approximation.

The same procedure followed in Sec. V may now be repeated but with these new functional forms. Equation (25) now yields

$$\mu_{l,i} = \sqrt{\sum_{j,k} w(r_{ij}) w(r_{ik}) f_l(r_{ij}) f_l(r_{ik}) P_l(\cos\ \theta_{jik})} \tag{32}$$

since we have, in analogy to Eq. (21)

$$\mu_{lm,i} = \sum_j Y_{lm}(\phi_{ij},\theta_{ij}) f_l(r_{ij}) w(r_{ij}) \tag{33}$$

One advantage to incorporating radial dependence in this way is that hydrostatic expansions of a lattice, for example, are now coupled with the effect of crystallographic distortions, in a manner analogous to the coupling of order parameters in Landau-Ginzburg theory.

B. Manifestations of these proposed forms in the present suite of interatomic potentials

Investigation of the literature reveals that a number of potentials already embody some aspects of the present for-

mulation. For example, the $l=0$ component of the energy reduces to the Morse pair potential[4] in the special case when $\mu_{0,i}^{0}=N$, there are N nearest neighbors included in $\rho_i(\mathbf{r})$ of equidistance r_{ij}, and the weighting function has an exponential form:

$$\mu_{0,i} = \sqrt{\sum_{j,k} w(r_{ij})w(r_{ik})P_0(\cos\ \theta_{jik})} = \sum_{jk} w(r_{ij})w(r_{ik})$$
$$= Nw(r_{ij}) = N\exp(-\beta r_{ij})E_{0,i} = F_{00}(N\exp(-\beta r_{ij}) - N)^2$$
$$\equiv A[\exp(-2\beta r_{ij}) - 2\exp(-\beta r_{ij})] \tag{34}$$

Similarly the Stillinger-Weber[26] potential for Silicon accesses the $l=2$ component

$$E_{1,i} = \sum_{j,k} w(r_{ij})w(r_{ik})\left(\cos\ \theta_{jik} - \frac{1}{3}\right)^2 \tag{35}$$

In this case $\frac{1}{3}$ is the value of the stationary point $\mu_{l,0}$ for the angle cosine, corresponding to the favored tetrahedral angle, 109.47°.

MEAM composes the local electron density (or *embedding* density) out of forms $l=0$ to $l=3$ determined using Eq. (32).[9] Although the link between the order parameter and the embedding density was not derived from any exact physical principles, it was considered conceptually reasonable to assemble angular components of the density according to the local crystallographic arrangement. An excellent discussion of the meaning associated with the MEAM parameters has been provided by Thijsse.[27] The NMEX procedure is thus distinct from MEAM in that the moments are not combined to produce some fictitious density, but rather are applied to the direct determination of the energy through the extensible functional form provided by the Taylor series expansion of Eq. (3) and the basis representation described in Eq. (19). At the same time, it should be recognized that MEAM has seen considerable success, in that the inclusion of density components according to Eq. (32) have been shown to significantly improve the performance of embedding potentials, to the point at which physically meaningful simulations can be performed even for complex materials such as plutonium metal.[28]

Analogous terms reappear in other off-shoots of the EAM, such as the embedded defect model, which utilizes $\mu_{2,i}$ as a means to capture the elastic properties of bcc metals.[29] In this case, Pasianot *et al.* derived this invariant by coupling a central-force model with the dipole tensor expression for defect-induced forces in a continuous medium. As in MEAM, this expression is described, without physical justification, as an angular contribution to the embedding density.

One additional parallel can be made, and this is to the expression for the bond order in the bond-order potential[30]

$$\Theta_{i,j} \propto \left\{\sum_{k,l} f_l(r_{ij},r_{ik})[P_l(\cos\ \theta_{jik}) + P_l(\cos\ \theta_{ijk})]\right\}^{-1/2} \tag{36}$$

where orders up to $l=6$ are required for f-electron materials, $l=4$ for d-electron materials and $l=2$ for s-p systems. In future work we plan to explore connections between the $\mu_{l,i}$ parameters and components of the electronic structure responsible for bonding and angular interactions.

VII. APPLICATION TO THE PHASE DIAGRAMS OF COPPER AND URANIUM

We have applied the NMEX formalism encapsulated by Eq. (30) and Eq. (32) to the cases of copper and uranium metal. Copper is a material that is presently well-described in general by EAM, and recently a variant of MEAM, called the multistate-modified embedded atom method (MS-MEAM) was applied to Cu.[31] While many properties of Cu were well-described by MS-MEAM, surface properties remained difficult to reproduce. The peculiar crystallographies exhibited by actinide metals, including U, have posed a problem to the existing suite of materials interaction potentials, by virtue of their lower symmetry expressions. A materials interaction potential, therefore, that acts upon a hierarchy of symmetry-adapted functions may have a greater degree of success in capturing these low symmetry preferences as well as providing a better description of surface properties.

A. Parameterization details

In order to develop the parameter sets for Cu and U, we utilize density-functional theory calculations performed using VASP.[32] Developing potentials in this way has become fairly popular due to the relatively high accuracy of DFT calculations, and their increasing efficiency for small, high-symmetry unit cells.[31,33,34] Since DFT calculations are most often limited to no more than a few hundred atoms, the development of interatomic potentials remains a high priority for those needing to simulate materials phenomena at the "mesoscale"—the size scale bridging nanometers to micrometers. In addition to reaching longer length scales, interatomic potentials can be used to simulate longer time scales.

The PW91 functional was used to incorporate exchange correlation,[35] and the projector-augmented wave method was used to approximate core electrons.[36] The k points and energy cutoff were chosen to allow convergence to within 5 meV. Within each self-consistent calculation energies were converged to 1×10^{-5} eV. Further details on density functional theory computations performed on Cu and U can be found in the literature.[31,37]

The proposed materials interaction potential, NMEX, requires a set of parameters for each atom type—here, Cu and U. The parameter set is composed of the coupling coefficients $\{F_{ll}\}$, the stationary points $\{\mu_l^0\}$, and parameters defining the weighting and radial functions, $w(r_{ij})$ and $f_l(r_{ij})$ respectively. To define these functions $f_l(r_{ij})$ and $w(r_{ij})$ exponential decays were assumed, thus allowing the two functions to be coupled into one, similarly to MEAM

$$f_l(r_{ij})w(r_{ij}) \equiv w_l(r_{ij}) = e^{-\beta_l(r_{ij}/r_0-1)} \tag{37}$$

r_0 is a reference distance, taken in MEAM to be the nearest-neighbor distance in the reference equilibrium fcc structure. We follow the same convention in this work. Thus a set of decay coefficients $\{\beta_l\}$ are required for each atom type, the constants r_0 for the reference fcc structures, and E_0 to set the

reference energies. Constraints were applied such that $\{F_{ll}\}$ and $\{\mu_l^0\}$ were required to be greater than zero, in accordance with the principles underlying their formulation: Namely, the second-order approximation implies that any perturbation to the moments from the ground-state configuration must be such that the energy is raised (negative coefficients F_{ll} would imply that the energy could be indefinitely lowered by a "runaway" of the moments to either very low or very large values); Since the μ_l values are positive by definition, the stationary points $\mu_{l,0}$ must also be positive. The weighting factors $\{\beta_l\}$ were required to be greater than 1.0 since their purpose is to localize the neighborhood about the given atom. An additional constraint could also be applied—namely, that μ_l^0 correspond to μ_l for the ground-state structure if it is truly known. Similarly E_0 could be constrained by the energy of the ground state also. However, it was found that this does not lead to an optimal parameterization for U and hence this constraint was relaxed. In the case of Cu, a good fit (i.e., just as accurate as the reference DFT energies)[38] can be obtained with this constraint, but a better one can be obtained if it is relaxed (see below). In both cases, the $\mu_{l,0}$ values are nonetheless close to the μ_l values obtained for the lowest-energy structure. It is considered that this difference may be due to: (a) limits placed on the maximum values of l considered herein (basis set incompleteness); (b) loss of information through use of rotational invariants; (c) neglect of coupling between symmetry states of different l; or (d) "hidden physics" such that optimal local arrangements corresponding to the true μ_l^0 values determined through unconstrained optimization are impossible to satisfy for all atoms in a crystallographic setting, and hence the ground-state structure has a different set of μ_l values.

During parameterization, the NMEX energies were determined by restricting the neighborhood to the minimal set of nearest neighbors. For symmetric phases this can be performed quite simply: In simple cubic (sc), fcc, diamond cubic (dc), and hcp the nearest neighbors all have identical environments and interatomic distances relative to the central atom. For the orthorhombic case of U there are 12 neighbors that can be described as NNs, having interatomic distances within a few percent of each other, although the symmetry of the system means that these neighbors are not equivalent, rather there are four symmetry related sets of three unique nearest neighbors.[39] In the bcc phase there are two sets of nearest neighbors. It is not clear how to include these NNs in the parameterization, hence the bcc phase is not used to fit the NMEX parameters. We shall consider this special case of the bcc phase of U later in this work.

B. Development of a materials interaction potential for copper

The training set for the NMEX Cu potential consists of 60 data points taken from the fcc, hcp, dc, sc, and fcc(111) phases, by evaluating the energies at a set of strains ranging from −20% to +10% relative to the fcc equilibrium bond length (r_0 is 2.574 Å). These points are shown in Fig. 1. Parameterization proceeded here and in the U case as follows: (1) The value E_0 was optimized to minimize the root-mean-square error in the NMEX energies compared to the DFT data shown in Fig. 1 with all F_{ll} set equal to zero; (2) Beginning with $l=0$, each of μ_l^0, β_l, and F_{ll}, as well as E_0 once more, were simultaneously optimized to minimize the same root-mean-square error; (3) Step (2) was repeated for increasing values of l up to $l=6$. The conjugate gradient method was used to minimize the root-mean-square error. We shall now describe the results of this process.

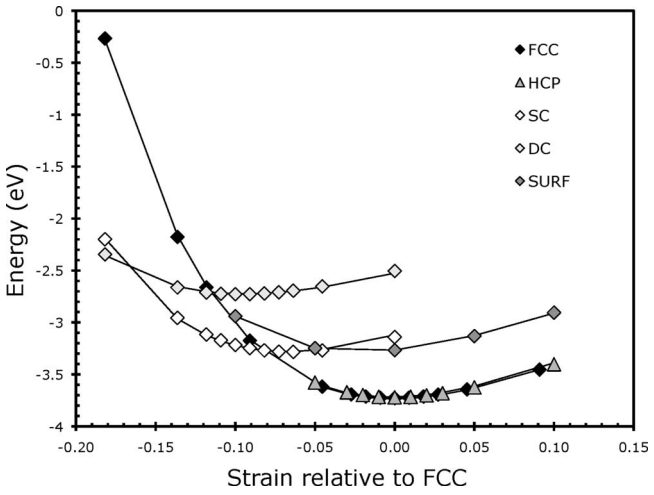

FIG. 1. Application of NMEX formalism to a series of hypothetical and actual crystal structures of Cu at various conditions of hydrostatic strain. Plotted data points indicate DFT data; lines connect the data points calculated using the optimized NMEX parameter set. Positive strain is tensile, negative is compressive.

In the absence of any representation of the local geometry, i.e., all of F_{ll} equal to zero, the root-mean-square error over the data set was 0.56 eV. Including F_{00} lowered this error to 0.28 eV. Including the term F_{11} reduced this error to 0.26 eV, while F_{22} was found to have no effect. Addition of F_{33} drops the error marginally to 0.18 eV, whereas the inclusion of F_{44} is found to lower the error by over an order of magnitude, to 0.007 eV. Subsequently F_{55} lowers the error to 0.002 eV, and F_{66} has no discernible effect. Since errors well within DFT accuracy are obtained at $l=4$ we present this parameter set in Table I.

As indicated by the exactness of the fit obtained using $l_{\max}=4$ the second-order framework using only diagonal terms F_{ll} can be considered sufficient to capture a variety of

TABLE I. NMEX parameters for Cu and U. E_0 for Cu is −3.85 eV and for U is −11.60 eV. F_{ll} is in units of $\times 10^{-2}$ eV.

l	0	1	2	3	4	5	6
Cu							
F_{ll}	1.91	6.16	0	4.95	2.32		
μ_l^0	11.70	0.00		1.28	3.49		
β_l	4.03	4.13		4.04	5.16		
U							
F_{ll}	3.47	1.11	60.49	1.98	0.478	0.341	0.014
μ_l^0	11.88	0.00	0.44	0.03	11.19	10.13	4.01
β_l	3.77	9.22	1.00	1.00	7.68	5.35	15.01

crystallographic environments. The *embedded topology* thus expressed by the bond-orientational order parameters μ_l appears to be sufficient to describe the interactions without the necessity of including a pair potential, as utilized in the embedded atom methods.[5] As highlighted earlier, under special conditions the NMEX term involving F_{00} in fact reduces to a commonly used pair potential.

The effect of each of the l components to the energy can be individually observed by systematically switching them "off" by setting $F_{ll}=0$. For instance removing the $l=4$ band leaves the curves for the fcc, dc, hcp and fcc(111) surface mostly unchanged, but significantly distorts the sc. Likewise, switching off $l=3$ maintains the integrity of the fcc, sc, surf, and hcp phases but dramatically distorts the placement and curvature of the dc phase. $l=2$ contributes nothing to the parameterization of the Cu crystallographic phases made herein, whereas it is found that $l=1$ is highly significant for obtaining the correct energies of the surface phase. Finally $l=0$ has a very broad impact upon obtaining the correct curvature and hence bulk moduli of all the crystalline phases studied herein. We will see similar, but somewhat different trends when we perform the same analysis for U shortly. As anticipated earlier through our qualitative analysis of the bond-orientational order parameters, each μ_l reveals something pertinent about the local crystallographic symmetry, which we have exploited for the purposes of developing an extensible materials interaction potential. The extensibility of this method is evidenced here by the ability to improve the accuracy of the fit systematically by the addition of higher order l terms in the basis expansions of the local atomic density distribution.

Earlier it was remarked that an additional constraint could be applied during parameterization, namely, requiring μ_l^0 and E_0 to match the properties of the ground-state crystallographic phase at the equilibrium volume. Applying this constraint leads to a potential still within the limits of expected DFT accuracy, but with a higher total error of 0.012 eV compared to 0.007 eV in the unconstrained case, both taken using a basis set up to $l=4$. As mentioned previously, the values of $\mu_{l,0}$ in the unconstrained case are similar to those of $\mu_{l,0}$ in the constrained case: {11.7,0,1.0,1.28,3.49} versus {12.0,0,0,0,2.29}, respectively.

C. Development of a materials interaction potential for uranium

Drawing from a database of 70 first-principles single-point energy calculations of various crystallographic phases for uranium following the methodology previously published,[37] we have evaluated the parameters $\{F_{ll}\}$, $\mu_{l,0}$, β_l, and E_0 for the spherical harmonics of order l up to $l=6$, as described above. The fcc equilibrium bond distance of 3.132 Å was used for r_0. The root–mean-square errors obtained during fitting were not as good as those obtained for Cu, and this is attributed to the greater sensitivity of this metal to the slight changes in crystallography embodied by the bond-orientational order parameters, μ_l. Without the use of the F_{ll} coupling parameters, optimizing E_0 alone produces a root-mean-square error of 2.96 eV. Including F_{00} lowers the error to 1.11 eV. Including the $l=1$ and $l=2$ bands reduces the error to 0.37 and 0.32 eV respectively. Incorporating $l=3$ reduces the error further to 0.13 eV, and F_{44} narrows this value down to 0.077 eV. A small incremental improvement in the fit arises from F_{55} (down to 0.076 eV) and finally, F_{66} yields a root-mean-square error of 0.045 eV. The final fit is shown in Fig. 2.

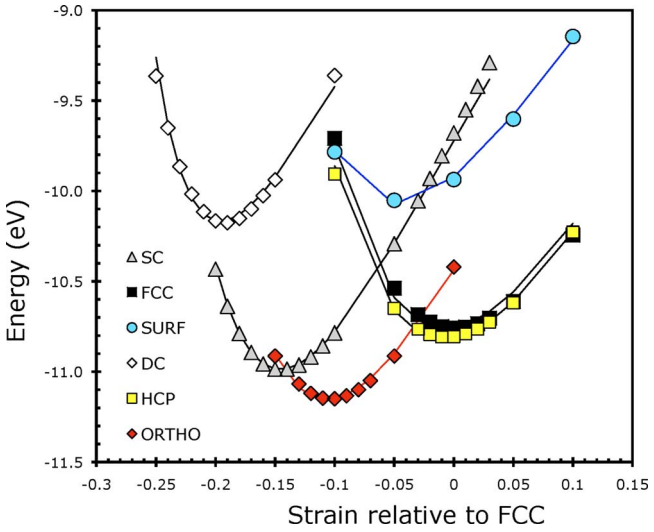

FIG. 2. (Color online) Application of NMEX formalism to a series of hypothetical and actual crystal structures of U at various conditions of hydrostatic strain. Plotted data points indicate DFT data; lines connect the data points calculated using the optimized NMEX parameter set. Positive strain is tensile, negative is compressive.

Constraining the values of μ_l^0 to match the moments of the equilibrium geometry of the orthorhombic phase is not as successful as in the case of Cu. The minimum root-mean-square error obtained using our optimization procedure is 0.18 eV and only the $l=0,1,3,4$ moments contribute. Visual inspection of the phase diagram obtained using this constraint shows that all the phases are reasonably described, with the exception of the simple cubic.

While not as successful as the Cu parameterization, the parameterization for U is still within DFT accuracy, and thus, reproduces the phase diagram to within the anticipated accuracy of the DFT calculations. However, the number of parameters now for U is significantly greater than that for Cu—a fact which should not be surprising considered the more complex crystallographic preferences demonstrated by this actinide series metal. As we considered earlier, it is possible to "breakdown" the contributions from each of the l modes to the overall phase diagram. Due to the difference in decay coefficients for a given l value between Cu and U we find that the contributions are somewhat different in each case. $l=3$ and $l=6$ strongly control the features of the dc phase for example, whereas $l=1$ and $l=2$ predominantly affect only the surface and orthorhombic phases. $l=0$ modifies the curvature of each of the phases when under tensile stress, whereas $l=4$ displaces the energy of all states except the dc with no change in curvature. For the case of U, turning off $l=5$ displaces the energies of the orthorhombic and hcp states with no real shifts in the curvature of these phases. As

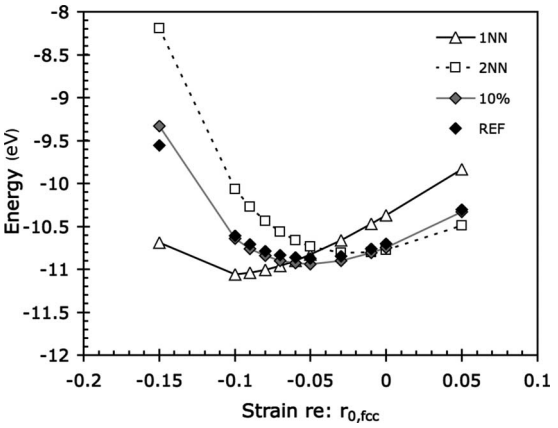

FIG. 3. Application of NMEX formalism to the bcc phase of uranium when first-nearest neighbors (1NN) and 2NN are included in the energy calculation. The NMEX energies are also given for the case when second-nearest neighbors are given a reduced treatment, corresponding to an additional 10% effective tensile strain (10%). The DFT values (REF) are also shown.

envisioned during construction of this model, and demonstrated previously for Cu, the μ_l order parameters provide a useful way of assigning energy contributions to different crystallographic features of the local atomic environment.

D. Consideration of screening: BCC uranium

It is instructive now to consider how the particular parameterization described above can be generalized to prepare a potential that is useful for atomistic simulation. The controlled environment of the atom utilized in the parameterization schemes is lost when a thermalized, dynamical environment is encountered, and there must therefore be introduced a sound scheme for determining which atoms are nearest neighbors and which ones are not, or whether there should be a gradual scheme by which neighbors in outer atomic shells should be considered. For the parameterization described in Figs. 1 and 2 the selection of nearest neighbors (i.e., the function $w(r_{ij})$) was simplified, as the generally high symmetries allowed nearest neighbors to be easily selected: in the case of the orthorhombic phase the 12 nearest neighbors were used. As discussed by Baskes,[9] the case of bcc complicates this choice. When we apply the NMEX parameter set derived for the cases of Fig. 2 to the bcc phase it is shown that inclusion of only first-nearest neighbors leads to a lower bound to the energy at compressive strains and an upper bound to the energy at tensile strains (Fig. 3). Compare this to the effect of using second-nearest neighbors (2NNs): in this case the NMEX energy is an upper bound to the true energy at compressive strains and a lower bound at tensile strains. These results suggest that the second-nearest neighbors should be included in the determination of the energy, but with a reduced contribution due to some kind of screening by the first-nearest neighbors. An unsophisticated way to demonstrate this is given in Fig. 3 in which is also plotted the NMEX energy for a 2NN bcc representation, but with the 2NNs treated as if they were displaced an additional 10% away from the central atom. The NMEX energy calculated using this simplistic treatment ends up being very close to the true energy. Exploration of appropriate screening techniques, including a physical basis for interatomic screening, will be made in a separate paper.

VIII. SUMMARY

In this work we have shown that there is a need for the development of a fundamental framework for materials interaction potentials, and provided one such framework based upon the concepts of localization through "embedding" and basis representations of the local crystallography. Beginning with the concept that the energy can be determined as a functional of the atomic density distribution function, we showed that successive approximations could be made to the total energy of the system through the technique of Taylor expansion. This approach was shown to be consistent with the density-functional theory that expresses system energy as a function of the electron density distribution function. Comparison of the approximations to the energy produced in this way with localized forms, separated atom wise, showed that relations existed, but that the functional forms were nontrivial; to avoid this difficulty a matrix representation was proposed, whereby the functions of atomic positions were replaced with matrix coefficients connecting basis functions. The basis of spherical harmonics was shown to be one method for representing the local crystallographic orientation about an atom, and the coefficients so derived were shown to be equivalent to the Steinhardt bond-orientational order parameters. By including radial-dependence, connections between the second-order energy approximations developed herein were made to various other forms of interatomic potential, including Morse, Stillinger-Weber, and the modified embedded atom method. Finally this second-order method was successfully shown to reconcile the phase diagrams for Cu and U, although further work will be required to extend this technique for generalized molecular dynamic or Monte Carlo simulations.

Areas requiring greater theoretical elaboration include the connection between matrix coupling constants and symmetries in the electronic structure of the materials, more rigorous examinations of the embedding assumption central to this work, and consideration of the physical basis by which first-nearest neighbors act to "screen" out the contribution of neighbors in more distance atomic shells. Once these questions are adequately solved, it is believed that the foundations will be laid for rigorously and systematically derived materials interaction potentials.

ACKNOWLEDGMENTS

The author is grateful to S. Lillard at Los Alamos National Laboratory for encouragement and assistance in funding this work, T. Lookman at Los Alamos National Laboratory for stimulating conversations regarding Landau theory, and M. Baskes, S. Valone, and R. Hoagland for discussions concerning the embedded atom method and interatomic potentials in general. Gratitude is also expressed toward the reviewers for their anonymous feedback and help in improv-

ing this manuscript. The author acknowledges the Seaborg LDRD Post-Doctoral Program for funding this work. Los Alamos National Laboratory is operated by Los Alamos National Security LLC for the National Nuclear Security Administration of the U.S. Department of Energy under Contract No. DE-AC52-06NA25396.

*cdtaylor@lanl.gov

[1] B. Harmon, J. Phys.: Conf. Ser. **16**, 273 (2005).
[2] J. E. Lennard-Jones, Proc. Phys. Soc. **43**, 461 (1931).
[3] M. Born and J. E. Mayer, Z. Phys. A: Hadrons Nucl. **75**, 1 (1932).
[4] P. M. Morse, Phys. Rev. **34**, 57 (1929).
[5] M. S. Daw, Phys. Rev. B **39**, 7441 (1989).
[6] J. H. Rose, J. R. Smith, F. Guinea, and J. Ferrante, Phys. Rev. B **29**, 2963 (1984).
[7] J. R. Smith, T. Perry, A. Banerjea, J. Ferrante, and G. Bozzolo, Phys. Rev. B **44**, 6444 (1991).
[8] M. S. Daw and M. I. Baskes, Phys. Rev. B **29**, 6443 (1984).
[9] M. I. Baskes, Phys. Rev. B **46**, 2727 (1992).
[10] K. W. Jacobsen, J. K. Nørskov, and M. J. Puska, Phys. Rev. B **35**, 7423 (1987).
[11] D. A. Papaconstantopoulos and M. J. Mehl, J. Phys.: Condens. Matter **15**, R413 (2003).
[12] J. C. Slater and G. F. Koster, Phys. Rev. **94**, 1498 (1954).
[13] A. C. T. van Duin, S. Dasgupta, F. Lorant, and W. A. Goddard III, J. Phys. Chem. A **105**, 9396 (2001).
[14] M. A. Iron, A. Heyden, G. Staszewska, and D. G. Truhlar, J. Chem. Theory Comput. **4**, 804 (2008).
[15] L. D. Landau and E. M. Lifshitz, *Statistical Physics, Course of Theoretical Physics*, 3rd ed. (Pergamon Press, New York, 1980).
[16] P. J. Steinhardt, D. R. Nelson, and M. Ronchetti, Phys. Rev. B **28**, 784 (1983).
[17] R. G. Parr, S. Liu, A. A. Kugler, and A. Nagy, Phys. Rev. A **52**, 969 (1995).
[18] M. J. Stott and E. Zaremba, Phys. Rev. B **22**, 1564 (1980).
[19] P. Hohenberg and W. Kohn, Phys. Rev. **136**, B864 (1964).
[20] C. J. Fennell and J. D. Gezelter, J. Chem. Phys. **124**, 234104 (2006).
[21] K. J. Strandburg, *Bond-orientational Order in Condensed Matter Systems, Partially Ordered Systems* (Springer-Verlag, New York, 1992).
[22] C. Chakravarty, Mol. Phys. **100**, 3777 (2002).
[23] E. Kaxiras, *Atomic and Electronic Structure of Solids* (Cambridge University Press, Cambridge, 2003).
[24] M. Kazhdan, T. Funkhouser, and S. Rusinkiewicz, in *Symposium on Geometry Processing* (ACM, New York, NY, USA, 2003).
[25] S. L. Frederiksen, K. W. Jacobsen, K. S. Brown, and J. P. Sethna, Phys. Rev. Lett. **93**, 165501 (2004).
[26] F. H. Stillinger and T. A. Weber, Phys. Rev. B **31**, 5262 (1985).
[27] B. Thijsse, Nucl. Instrum. Methods Phys. Res. B **228**, 198 (2005).
[28] M. I. Baskes, Phys. Rev. B **62**, 15532 (2000).
[29] R. Pasianot, D. Farkas, and E. J. Savino, Phys. Rev. B **43**, 6952 (1991).
[30] S. R. Nishitani, P. Alinaghian, C. Hausleitner, and D. G. Pettifor, Philos. Mag. Lett. **69**, 177 (1994).
[31] M. I. Baskes, S. G. Srinivasan, S. M. Valone, and R. G. Hoagland, Phys. Rev. B **75**, 094113 (2007).
[32] G. Kresse and J. Furthmuller, Phys. Rev. B **54**, 11169 (1996).
[33] M. I. Baskes, S. P. Chen, and F. J. Cherne, Phys. Rev. B **66**, 104107 (2002).
[34] G. Grochola, S. P. Russo, and I. K. Snook, J. Chem. Phys. **123**, 204719 (2005).
[35] J. P. Perdew, J. A. Chevary, S. H. Vosko, K. A. Jackson, M. R. Pederson, D. J. Singh, and C. Fiolhais, Phys. Rev. B **46**, 6671 (1992).
[36] G. Kresse and D. Joubert, Phys. Rev. B **59**, 1758 (1999).
[37] C. D. Taylor, Phys. Rev. B **77**, 094119 (2008).
[38] The errors in DFT calculations are no better than the "chemical accuracy" of 1 kcal/mol or about 0.05 eV.
[39] A. S. Wilson and R. E. Rundle, Acta Crystallogr. **2**, 126 (1949).